Paper No.
26

CORROSION 98

MODELING THE DIFFUSION EFFECTS THROUGH THE IRON CARBONATE LAYER IN THE CARBON DIOXIDE CORROSION OF CARBON STEEL

S. RAJAPPA, R. ZHANG AND M.GOPAL
NSF, I/UCRC CORROSION IN MULTIPHASE SYSTEMS CENTER
DEPARTMENT OF CHEMICAL ENGINEERING
OHIO UNIVERSITY, ATHENS, OHIO, USA

ABSTRACT

A mechanistic model was developed for predicting carbon dioxide corrosion rates of carbon steel pipes in multiphase flow conditions. The model incorporates the chemistry, thermodynamics of carbon dioxide dissolution, multiphase mass transfer, electrochemical kinetics on the metal surface and the presence of a corrosion product film. The predicted corrosion rates show good agreement with the experimental results.

Keywords: **Corrosion, pH, mass transfer coefficients, coupons, SEM**

INTRODUCTION

The depletion of accessible oil resources has directed oil production to remote areas, such as the sub-sea and Alaska. The main products from the oil wells are oil and natural gas. For sub-sea production, offshore platforms have been used to separate the oil and gas which are then transported onshore using single phase pipelines. It is not feasible or economical to separate the oil and gas at each well site and hence the mixture of oil and gas are transported together many miles to a central gathering station where the phases are separated. The presence of carbon dioxide causes internal sweet corrosion due to the formation of weak corrosive carbonic acid with salt water. This significantly increases corrosion rates in carbon steel pipelines. Since most pipelines are located in inaccessible

places, maintenance operations are very difficult and expensive. It is imperative that proper design and operating conditions be maintained to minimize corrosion. For the selection of appropriate design parameters it is imperative to quantify corrosion. Moreover, it is important to determine operating conditions such as temperature, pressure, velocities and oil/water fractions under which corrosion is minimized.

Corrosion occurs due to the interaction of the liquid and metal ions forming discrete electrochemical cells. Two factors that significantly affect the rate of this reaction are the mass transfer of ions from the flowing liquid to the metal wall and thickness of the corrosion product, on the surface of the metal. In order to understand the mechanisms involved with the formation of the iron carbonate layer, which is a significant factor in controlling the diffusion rate, an extensive literature survey is presented in the following section.

Corrosion Mechanisms

de Waard and Milliams[1] (1975) studied the mechanisms of carbon dioxide corrosion of carbon steel under various conditions of pH, temperature and pressure.

Corrosion mechanisms have been investigated by Ikeda[4] (1985), Videm and Dugstad[5] (1989), de Waard et al.[6] (1991) and de Waard and Lotz[7] (1993).

Dayalan et al.[2] (1995) proposed a mechanistic model for the carbon dioxide corrosion of steel in pipe flow. They suggested the following steps

1. Formation of reactive species in the bulk
2. Transportation of reactants (bulk to surface)
3. Electrochemical reactions at the surface
4. Transportation of products (surface to bulk)

They suggested that three species (H^+, H_2CO_3 and HCO_3^-) undergo reduction at the metal surface and contribute to corrosion. Their study was limited to brine with 3% NaCl solution. There was no evaluation of the corrosion product film and they limited their work to 2.5 cm pipelines, with no comparison with experimental data for large diameter pipelines.

In this study, the model simplification involves reducing the number of cathodic reactions relevant to the corrosion process. Only the reduction of hydrogen ions is considered according to Herce et al.[3] (1995) since they combined the effects of fluid flow with pH to define hydrogen ion flux which they related to corrosion rate under a variety of conditions. Hence, only two reactions that are of interest in this corrosion model are given below and they are the oxidation of iron to the ferrous ion as the anodic reaction and the reduction of the hydrogen ion as the cathodic reaction.

Cathodic reaction	$2H^+$	+	$2e^-$	$\Leftrightarrow$	H_2			**(1)**
Anodic reaction	Fe			$\Leftrightarrow$	Fe^{2+}	+	$2e^-$	**(2)**

Previously a corrosion model has been presented (Zhang et al[18]. 1997) without the effect of corrosion product layer as shown in Figure 1. In the case where a corrosion film forms, the mass transfer is described schematically in Figure 2. Here the mass transfer region exists between a corrosion layer and the bulk solution. As before species move through previously modeled regions, but the additional transport through the corrosion film must be considered. For simplicity only the movement of the ferrous ion and the hydrogen ion will be considered in this layer since only these two ions are of interest for the surface reactions.

Corrosion product layer

In sweet corrosion, the corrosion products formed on the pipe wall are iron carbonate and iron bicarbonate but iron bicarbonate has not been observed from experimental studies and decomposes to iron carbonate and carbonic acid at higher temperatures (de Waard and Milliams[1] -1975). The iron carbonate formed can form a protective film on the pipe wall depending on the pH of the solution, temperature, pressure and flow rate. The simplified overall reactions are

CO_2	+	H_2O	$\Leftrightarrow$	H_2CO_3				**(3)**
Fe	+	$2H_2CO_3$	$\Leftrightarrow$	$Fe(HCO_3)_2$	+	H_2		**(4)**
Fe	+	H_2CO_3	$\Leftrightarrow$	$FeCO_3$	+	H_2		**(5)**

The iron bicarbonate decomposes at higher temperatures forming the main corrosion product, iron carbonate. This reaction is given by

$$Fe(HCO_3)_2 \Leftrightarrow FeCO_3 + H_2CO_3 \quad (6)$$

de Waard and Milliams[1] (1975) showed that the solubility of iron carbonate which is usually the main corrosion product is low and decreases with increase in temperature. The iron carbonate dissolves in the solution until its solubility limit is reached. Thereafter the solution becomes supersaturated and the iron carbonate precipitates on the metal wall.

Autoclave studies by Efird and Jasinski[8] (1989) showed that crude oil, inspite of being non-corrosive to steel, does have a significant effect on the corrosion of steel when mixed with brine. They also showed that the degree of corrosion product protectiveness depends upon the crystalline size of the corrosion products and hence extrapolation of the studies with brine to field conditions can lead to gross errors.

Tomson et al.[9] (1991) have shown that ferrous carbonate precipitation kinetics is extremely temperature sensitive. At low temperatures (< 60°C) ferrous carbonate does not adhere to the surface and is transported away from the surface by fluid movement. At intermediate temperatures (60°C - 150 °C) a loosely adherent film causes deep pitting and

extremely high corrosion rates. At even higher temperatures (>150°C) tight adherent films are formed. Quenched and tempered materials are not easily corroded as low carbon steels, thus severe pitting may be observed in low carbon materials

Studies by Heuer[10] (1996) showed that this pitting corrosion is not only dependent on temperature but on flow rate and specimen metallurgy.

Dugstad[11] (1992) found that the super saturation level of iron carbonate and the pH is dependent on the water volume to steel ratio and the temperature. Protective films are not easily formed as precipitation rate of iron carbonate is a slow and a temperature dependent process. Also under supersaturated conditions, it takes 20 to 40 hours to cover the metal surface with the protective iron carbonate layer.

Vuppu[12] (1994) performed studies on the characteristics of the protective iron carbonate film formed on the metal surface under various conditions of temperature, pressure, oil/water fraction and flow conditions. He found from SEM studies, that at temperatures below 60°C, the corrosion deposit formed under full pipe flow conditions was of uniform thickness with long cracks in it. The deposit turns more crystalline with increase in temperature and pressure. Also, at intermediate oil/water compositions, the corrosion products are loose and porous and the formation of protective iron carbonate scales was found to occur at temperatures >70°C for brine. However for multiphase oil/salt water flows, such formation of protective scales was not found.

Videm and Kvarekvaal (1996) showed that the most important surface changes induced by corrosion of an initially smooth and uncorroded steel are changing the area of the reacting surface, carbide accumulation at the surface, formation of carbonate films, flow induced removal of corrosion films and formation and breakdown of sulfide film in environments with sulfides. In their experiments specimens with one surface freshly ground and another being the original cold rolled steel were used. They concluded from their study that corrosion has "good memory" for what has happened earlier and that experiments must be strictly controlled in order not to be ruined by pre-corrosion.

Nesic et al[13]. (1995) shed more light on the anodic reaction mechanism in CO_2 corrosion of mild steel. They used potentiodynamic sweep and galvanostatic measurements for their electrochemical measurements. They found distinct but different anodic mechanisms for iron dissolution in CO_2 solutions for both pH<4.0 and for pH>5.0. In the intermediate area there seems to be a transition from one mechanism to another.

Nesic et al. (1996) explained influence of the iron content in the corrosive medium. They found that if the iron content in the test medium is high from the moment of immersion of freshly polished specimens, iron carbonate can precipitate on the metal, and the layer is protective. If the iron content in the medium becomes high only after an initial phase of corrosion leading to the formation of a porous cementite layer, then internal acidification prevents further precipitation of iron carbonate in contact with the metal. The

layer is then unprotective, and even enormous amounts of super saturations cannot subsequently render it protective.

Heuer[10] (1996) reported the effect of temperature, pressure, Froude number and oil cut on the corrosion products formed in horizontal multiphase flow. He found that coupons run under full pipe flow have much thicker films than specimens exposed to slug flow. The average thickness in full pipe flow is about three times greater than that for slug flow. The average thickness of the corrosion product layer found on the surfaces of coupons exposed to slug flow conditions was about 6 to 14 microns, which is smaller than the average thickness for full pipe flow conditions (36 to 44 microns). This indicates the possible stripping of the protective film of corrosion products on the metal surface, due to higher levels of shear stress and turbulence, under slug flow conditions.

Model Development

In a previous study (Zhang et al.[18], 1997) the calculation of bulk concentration of various ions and the calculation of pH were given.

In this case the pH was calculated using the relation

$$pH = -Log\ [\ a_{H^+}\ ] \tag{7}$$

For the calculation of a_{H^+} the following quadratic equation was used

$$\frac{1}{\gamma_{H^+}} a_{H^+}{}^2 + \lambda a_{H^+} + \left[- \frac{K_1 CO_2 \cdot a_{CO_2}}{\gamma_{HCO_3}} - \frac{K_W}{\gamma_{OH}^-} \right] = 0 \tag{8}$$

Mass Transfer Coefficients

In order to calculate the mass transfer flux of the species it is necessary to compute the mass transfer coefficients of the species. In this study the following expression was used

$$K_{mt} = \frac{4.586 \left(\frac{Vmax}{Vavg}\right) f\, Re\, D\, (Sc)^{1/3}}{8\, d} \tag{9}$$

where V_{max} = Maximum velocity in the pipe in m/s,
V_{avg} = Average velocity in the pipe in m/s

The Moody friction factor can be calculated by using the correlation of Haaland (1991)

$$f^{-1/2} = -1.8 \log_{10} \left[\frac{6.9}{Re} + \frac{(e/d)^{1.11}}{3.7} \right] \quad (10)$$

Where e = Roughness of the pipe, d = diameter of the pipe and Re = Reynolds number.

Diffusion coefficient

The mass transfer coefficient requires diffusivity calculations. The diffusion coefficients of the ions can be calculated with the aid of the Nernst - Einstein relation

$$D_i = \frac{\lambda_i R T}{F^2 Z_i} \quad (11)$$

Where D_i = Diffusion coefficient, λ = ionic conductivity, R = universal gas constant, T = temperature (°K) and Z = charge of the ion.

From the results of Xie[19] (1997), it was found that the diffusivities of D, 2D and 3D were used for 40, 60 and 80 °C respectively for brine and oil/water flow conditions, to predict corrosion rates since mass transfer rate increases greatly with temperature.

Modeling of corrosion with corrosion product layer

The reactant H^+ passes from the bulk solution to the metal surface through a mass transfer region, and the products, Fe^{2+} and CO_3^{2-} move from the metal surface towards the bulk solution. In the case where a corrosion film forms, there is a corrosion product layer which is composed of the porous media between the metal surface and the bulk solution. Species move through the bulk as before but the additional diffusion and transport through the corrosion film must be considered. For simplicity, only the movement of the ferrous ion and hydrogen ion will be considered.

Assuming no chemical reaction, applying a mass balance over the differential region of corrosion product film from z to z + Δz gives that at steady state :

$$N_{Az}|_{z+\Delta z}\, 2\pi(r - z - \Delta z)l - N_{Az}|_{z}\, 2\pi(r - z)l = 0 \qquad (12)$$

where, N_{Az} = molar flux of species A at z direction (mol/m^2/s)
r = radius of the pipe (m)
l = length of the pipe (m)

Rearranging gives

$$\frac{N_{Az}|_{z+\Delta z} - N_{Az}|_{z}}{\Delta z} = \frac{N_{Az}|_{z+\Delta z}}{r - z} \qquad (13)$$

Taking the limit as Δz approaches zero gives

$$\frac{dN_{Az}}{dz} = \frac{N_{Az}}{r - z} \qquad (14)$$

Integrating with respect to z gives

$$N_{Az} = \frac{C}{r - z} \qquad (15)$$

where, C = constant

At steady state, the rate of mass transfer is equal to the electrochemical reaction rate at the metal surface. The boundary condition is described as following :

at $z = 0$, $N_{Az} = C/r = R_A$

where, R_A = electrochemical reaction rate of species A (mol/m^2/s)
hence, $C = R_A\, r$

$$N_{Az} = \frac{R_A r}{r - z} \qquad (16)$$

For Fe^{2+} :

$$N_{Fe^{2+}z} = \frac{R_{Fe^{2+}} r}{r - z} \tag{17}$$

where, $N_{Fe^{2+}z}$ = molar flux of Fe^{2+} ($mol/m^2/s$)
$R_{Fe^{2+}}$ = electrochemical reaction rate of Fe^{2+} ($mol/m^2/s$) = i_a /2F
i_a = anodic potential (amp/m^2)
F = Faraday constant

Similarly for H^+ :

$$N_{H^+z} = -\frac{R_{H^+} r}{r - z} \tag{18}$$

where, N_{H^+z} = molar flux of H^+ ($mol/m^2/s$)
R_{H^+} = electrochemical reaction rate of H^+ ($mol/m^2/s$) = i_c /F
i_c = cathodic potential (amp/m^2)

For steady state, $i_a = i_c$, and gives :

$$N_{H^+z} = -2N_{Fe^{2+}z} \tag{19}$$

The ratio of molar flux of $H^+$and Fe^{2+} is -2. From the anodic and cathodic reactions, it can be seen that 1 mole Fe^{2+} needs 2 moles H^+ to react on each other and the ionic molar fluxes of Fe^{2+} and H^+ are in the opposite directions.

According to Fogler[19](1986), the total molar flux of A, N_{Az} , is the result of two contributions: the molecular diffusion flux, produced by a concentration gradient, and the flux resulting from the convection of the fluid.

$$N_{Az} = -c D_{AB} \frac{dx_A}{dz} + x_A (N_{Az} + N_{Bz}) \tag{20}$$

where,

N_{Az} = molar flux of A ($mol/m^2/s$)
N_{Bz} = molar flux of B ($mol/m^2/s$)
D_{AB} = diffusivity of A in a binary system (m^2/s)
x_A = mole fraction of A
c = molar density of solution (mol/m^3) = ρ/M
ρ = density of solution (kg/m^3)
M = molecular weight of solution (kg/kmol)

For Fe^{2+} :

$$N_{Fe^{2+}z} = -c\,D_{Fe^{2+}}\frac{dx_{Fe^{2+}}}{dz} + x_{Fe^{2+}}(N_{Fe^{2+}z} + N_{H^{+}z}) \tag{21}$$

When Eq. 19 is substituted into Eq. 21, the following expressions were obtained :

$$N_{Fe^{2+}z} = -cD_{Fe^{2+}}\frac{dx_{Fe^{2+}}}{dz} - x_{Fe^{2+}}N_{Fe^{2+}z} \tag{22}$$

hence,

$$N_{Fe^{2+}z}\,dz = -\frac{cD_{Fe^{2+}}}{1 + x_{Fe^{2+}}}\,dx_{Fe^{2+}} \tag{23}$$

When Eq. 17 is substituted into Eq. 23 , the following expression was obtained

$$\frac{i_a r}{2F(r - z)}\,dz = -\frac{cD_{Fe^{2+}}}{1 + x_{Fe^{2+}}}\,dx_{Fe^{2+}} \tag{24}$$

Integrating with respect to z from 0 to δ, with the boundary conditions

at z=0, x_{Fe}^{2+} = FeS/c
at z=δ, x_{Fe}^{2+} = FeL/c

and integrating with respect to x_{Fe}^{2+} from metal surface to the edge of the corrosion film, gives :

$$\frac{i_a r}{2F}\ln(1 - \frac{\delta}{r}) = cD_{Fe^{2+}}[\ln(1 + \frac{FeL}{c}) - \ln(1 + \frac{FeS}{c})] \tag{25}$$

where,

δ	=	thickness of the corrosion film (m)
FeL	=	Film concentration of Fe^{2+} (mol/m^3)
FeS	=	metal surface concentration of Fe^{2+} (mol/m^3)
D_{Fe}^{2+}	=	diffusivity of Fe^{2+} through corrosion film (m^2/s)
c	=	molar density of solution = ρ /M (mol/m^3) =69444.4mol/m^3 for brine
ρ	=	density of solution (kg/m^3)
M	=	molecular weight of solution (kg/kmol)

Similarly for H^+ :

$$N_{H^+z} = -c D_{H^+} \frac{dx_{H^+}}{dz} + x_{H^+}(N_{Fe^{2+}z} + N_{H^+z}) \tag{26}$$

Substitute Eq.(19) into Eq.(26), gives :

$$N_{H^+z} = -c D_{H^+} \frac{dx_{H^+}}{dz} + \frac{1}{2} x_{H^+} N_{H^+z} \tag{27}$$

$$N_{H^+z}\, dz = -\frac{cD_{H^+}}{1 - 0.5\, x_{H^+}}\, dx_{H^+} \tag{28}$$

Substitute Eq.(18) into Eq. (28), gives :

$$\frac{i_c r}{F(r - z)}\, dz = \frac{cD_{H^+}}{1 - 0.5\, x_{H^+}}\, dx_{H^+} \tag{29}$$

Integrating with respect to z from 0 to δ, and the boundary conditions are described as following,

at z=0, $x_{H+} = H^+S/c$
at z=δ, $x_{H+} = H^+L/c$

and integrating with respect to x_{H+} from metal surface to the edge of the corrosion film, gives :

$$\frac{i_c r}{F} \ln(1 - \frac{\delta}{r}) = 2\, cD_{H^+} [\ln(1 - \frac{0.5H^+L}{c}) - \ln(1 - \frac{0.5H^+S}{c})] \tag{30}$$

where, H^+L = film concentration of H^+ (mol/m^3)
H^+S = metal surface concentration of H^+ (mol/m^3)

Eqs.(25) and (30) are simplified by using the series expansions :

$$\ln(1 + x) = x - \frac{x^2}{2} + \frac{x^3}{3} - \frac{x^4}{4} + ... + (-1)^{n+1} \frac{x^n}{n} + ... \tag{31}$$

@ $-1 \le x < 1$

$$\ln(1-x) = -(x + \frac{x^2}{2} + \frac{x^3}{3} + \frac{x^4}{4} + ... + \frac{x^n}{n} + ...) \qquad (32)$$

@ $-1 \leq x < 1$

For Fe^{2+}, $0 < \delta/r << 1$, $0 < FeL/c << 1$ and $0 < FeS/c << 1$, so keeping only one term in series expansion, Eq.(25) gives:

$$-\frac{i_a}{2F}\delta = D_{Fe^{2+}}(FeL - FeS) \qquad (33)$$

Hence,

$$FeL = FeS - \frac{i_a \delta}{2F\, D_{Fe^{2+}}} \qquad (34)$$

For H^+, $0 < \delta/r << 1$, $0 < H^+L/2c << 1$ and $0 < H^+S/2c << 1$, keeping only one term in series expansion, Eq(30) gives:

$$\frac{i_c}{F}\delta = D_{H^+}(H^+L - H^+S) \qquad (35)$$

$$H^+L = H^+S + \frac{i_c \delta}{F\, D_{H^+}} \qquad (36)$$

$$i_c = i_a = i_{corr} \qquad (37)$$

For iron, Corrosion rate (mm/year) = i_{corr} (amp/cm^2) * (1.16 * 10^4) and

$$F\,K_{mt,H^+}(H^+b - H^+L) = i_c \tag{38}$$

$$2\,F\,K_{mt,Fe^{2+}}(FeL - Feb) = i_a \tag{39}$$

where,

Feb	=	bulk concentration of Fe^{2+}	(mol/m^3)
FeL	=	Film concentration of Fe^{2+}	(mol/m^3)
H^+b	=	bulk concentration of H^+	(mol/m^3)
H^+L	=	film concentration of H^+	(mol/m^3)

Diffusivity in porous corrosion film

According to Satterfield[16](1980), pore diffusion may occur by bulk diffusion. He suggested that the bulk diffusion coefficient for porous media, $D_{12,eff}$, be expressed as

$$D_{12,eff} = \frac{D_{12}\theta}{\tau} \tag{40}$$

where,

θ	=	void fraction
τ	=	tortuosity factor

Experimental measurements on a variety of commercial catalysts show that in many cases, values of τ is in the range of 2 to 7, values of θ vary from about 0.3 to 0.7.

If the pores are large and gas relatively dense (or if the pores are filled with liquid), the process is that of bulk or ordinary, *diffusion*. In this study, the pores of corrosion product film are large and the corrosion film are not composed of the traditional crystals, hence, $\theta/\tau = 1.0$ is investigated for the porous corrosion film.

According to Fogler[17](1986), the total molar flux of A, N_{Az}, is the result of two contributions, the molecular diffusion flux, produced by a concentration gradient, and the flux resulting from the convection of the fluid. If the pores of corrosion product film are wide and the film is thick, the second contribution cannot be neglected. In addition to

natural convection, forced convection exists and plays an important role in fully developed turbulent pipe flow conditions. The mass transfer in large pores is the mixture of mass transfer by diffusion (including diffusion through liquid and solid) and convection (combination of natural and forced convection). Incorporating mass transfer by the effects of forced convection and diffusion through solid into the total molar flux, θ/τ = 5, 10, and 15 are tested for the porous corrosion film through increasing the rate of mass transfer by diffusion through liquid.

EXPERIMENTAL SET UP

The entire system in which the experiments were carried out is made of 316 stainless steel and is designed to withstand a maximum pressure of 1500 psi. A predetermined oil-water mixture is stored in a 1.2 m^3 tank. The liquid is pumped by a 5.2KW stainless steel, centrifugal pump into a 7.62 cm ID, 0.95 cm thick pipeline from where it flows into the 10 m long, 10.16 cm ID and 0.95 cm thick test section. The test section contains two openings which are used for the introduction of Electrical Resistance probes and Coupon holders for corrosion rate measurements and for SEM studies. The experimental setup has been discussed extensively in previous papers published from the center.

RESULTS AND DISCUSSION

Experiments were conducted for a water cut of 40% at 80 °C and 0.79 MPa for full pipe flow conditions (Velocity = 1.0 m/s) with various iron concentrations (100 and 200 ppm).

The experiments were conducted for about 72 hours. It was seen that when the coupons were examined under the SEM a thick layer of iron carbonate was precipitated on the surface of the coupon as shown in Figure 3. The layer was even thicker as seen in Figure 4. when the iron content was raised from 100 to 200 ppm. It was noticed that, though the corrosion rate had reached an equilibrium value there was no marginal drop in the corrosion rate and there was hardly any difference when the data was compared with the data obtained from experiments conducted under very less iron concentrations. Apart from the coupon studies, the pH was also measured for various experiments and it was found that an increase in the iron concentration did not change the pH of the solution. This explains the reason why there is no drop in the corrosion rates as a drop in the corrosion rate would increase the pH closer to 7.0. This fact also corroborates an important assumption, which is made in the development of the model that the dissolution reaction of iron into the solution does not significantly affect the bulk pH.

Temperature Dependence of Corrosion Rate

It is seen that the predicted corrosion rate increases greatly with temperature for non-scaling conditions. For example, for brine, at a pressure of 0.79MPa, the predicted corrosion rates are 10.1, 18.2 and 23.9 mm/year for 40, 60 and 80^{0}C respectively, while the corresponding experimental results are 9.4, 25.47 and 22.61 mm/yr. This tendency reveals the scaling temperature is lower than 80^{0}C for brine.

From Figure 5, it is seen that model predicts well the experimental results by using 1×D for diffusivity calculations at 40^0C. From Figure 6, the model results seem to slightly under predict the experimental data, but is reasonable compared with experimental observations by using 2×D for diffusivity calculations at 60^0C. From Figure 7, it is seen that the model results are very close to the experimental results by using 3×D for diffusivity calculations at 80^0C. except two points which are at higher pressure(0.79MPa) for oil/water flows.

Corrosion film effect

For the presence of a corrosion product film, the values of the ratio of void fraction and tortuosity θ/τ = 1, 5, 10 and 15 are chosen, for the calculation of the diffusivity in porous corrosion film. These values are chosen due to the large pore size.

It is seen that corrosion rate increases with the value of the ratio of void fraction and tortuosity which is represented by θ/τ, since the rate of mass transfer through the porous product film increases with θ/τ. For example, at 40^0C, film thickness of 30 microns, for brine, at a pressure of 0.79MPa, the predicted corrosion rates are 3.0, 6.8, 8.2 and 8.7 mm/year for four different values of θ/τ(1, 5, 10 and 15) respectively, and for 20%oil-80%saltwater, at the same condition, the predicted corrosion rates are 3.5, 10.3, 13.7 and15.3 mm/year respectively with increasing θ/τ.

From Figure 8. It can be seen that the model predicts well the experimental results at θ/τ of 15 for 40, 60 and 80^0C, at film thickness of 30 to 40 microns. The comparison with experimental corrosion rates reveals that θ/τ of 15 can represent the total mass transfer which includes total diffusion (diffusions through both liquid and solid) and total convection (both natural and forced convection) contributions through the porous corrosion product film in which the pores are wide or large and film is thick in fully developed turbulent pipe flow conditions.

Choosing the value of θ/τ of 1 results in under prediction of the experimental data. It indicates that the diffusion contribution cannot represent the total mass transfer through the porous film in which the pore radii is small, the convection contribution to the total mass transfer also needs to be considered.

The effect of the film thickness on the corrosion rate was also studied. Film thickness of 30 and 40 microns were studied. These are shown from Figure 8 through 13.

Effect of velocity

It is seen that the corrosion rate increases with velocity but the increase is not linear. The corrosion rate versus velocity plot is a curve with the slope continuously decreasing as the velocity increases which is similar to Dayalan et al[2] 's studies on the effect of velocity. The corrosion rate should increase nearly linearly with velocity for cases where

the corrosion processes are mass transfer controlled. Figure 14. shows the effect of velocity on predicted corrosion rate for 0.13 MPa carbon dioxide partial pressure, at temperatures of 40, 60 and 80°C for ASTM seawater in 4 " pipe. It is seen that the corrosion process becomes reaction rate controlled at a velocity of 15 m/s for 40°C which can be described as the limiting velocity, which goes up with increase in temperature since the reaction rate increases much more quickly than the mass transfer rate. For example a temperature rise from 40°C to 60 °C increases the reaction rate constants to about 10 times while the mass transfer coefficient increases only about 2 times.

CONCLUSIONS

A mechanistic model is presented for the prediction of sweet corrosion in two phase oil/salt water flows. The model incorporates the chemistry of the salt, thermodynamics of carbon dioxide dissolution and dissociation, two phase mass transfer, electrochemical kinetics on the metal surface and the presence of a corrosion product film. The model follows the same steps as described by Dayalan[2] (1995) but the number of cathodic reactions are reduced. The calculation of pH includes the activity and activity coefficient of hydrogen ion and this is related to the concentrations of other ions in solution. Mass transfer coefficients are calculated using the Veith et al[17]. expression as the predicted corrosion rates calculated using this expression shows good agreement with the experimental results but mass transfer coefficients calculated using mixture properties result in under prediction of corrosion rates. The model predicts well the experimental results by using the value of the ratio of void fraction and tortuosity (15) for film thickness of 30 to 40 microns. The value represents both total diffusion (Diffusion through liquid and solid) and total convection (combination of natural and forced convection) through the porous corrosion product film in which the pores are wide or large and the film is thick.

REFERENCES

1. de Waard, C and Milliams, D. E, "Carbonic acid corrosion of steel", Corrosion, Vol. 31, No.5, pp. 177, 1975.
2. Dayalan et al., "Modeling carbon dioxide corrosion of carbon steel in pipe flow", Corrosion '95, 118/1 – 118/24, 1995.
3. Herce et al., "Effects of solution chemistry and flow on the corrosion of carbon steel in sweet production", Corrosion '95, 111/1 – 111/26, 1995.
4. Ikeda, A, Ueda, M and Mukai, S, "CO_2 behavior of carbon and Cr steels", Advances in CO_2 corrosion, Vol. 1, NACE, Houston, TX, 1985.
5. Videm, K and Dugstad, A, "Corrosion of carbon steel in an aqueous carbon dioxide environment. Part 1: Solution effects", Material Performance, 63 – 67, March 1989.
6. de Waard et al., "Prediction model for CO_2 corrosion engineering in wet gas pipelines", Corrosion, Vol. 47, No. 12, pp 976, 1991.
7. de Waard et al., "Prediction model for CO_2 corrosion of carbon steel", Corrosion '93, NACE, 69, 1993.

8. Efird, K. D and Jasinski, R. J., "Effect of crude oil on corrosion of steel in crude oil/brine production", Corrosion, 45(2), 165 – 171, 1989.
9. Tomson et al., "How ferrous carbonate kinetics impacts oil field corrosion", SPE '91, 257-262, 1991.
10. Heuer, K. J, "Preparation and examination of $FeCO_3$ and Fe_3C films found in CO_2 corrosion of low carbon steel", MS thesis – University of Illinois at Urbana Champaign, 1996.
11. Dugstad, A, "The importance of iron carbonate super saturation on the carbon dioxide corrosion of the carbon steels", Corrosion '92, NACE, 14, 1992.
12. Vuppu, A. K, "Study of carbon dioxide corrosion of carbon steel pipes in multiphase flow", MS thesis – Ohio university, Athens, 1994.
13. Nesic et al., "An electrochemical model for prediction of carbon dioxide corrosion", Corrosion '95, 131/1 – 131/26, 1995.
14. de Waard et al., "Influence of liquid flow velocity in CO_2 corrosion of carbon steel", Corrosion '95, 128/1 – 128/15, 1995.
15. Vieth, W. R, Porter, J. H and Sherwood, T. K, Ind. Eng. Chem. Fundamentals 2.1, 1963.
16. Satterfield, "Heterogeneous catalysts in practice", 1980
17. Scott fogler, H, "Elements of chemical reaction engineering", 1986
18. R. Zhang, M. Gopal and W. P. Jepson, "Development of a Mechanistic Model for Predicting Corrosion Rate in Multiphase Oil/Water/Gas Flows", Corrosion '97, NACE, Paper No. 601, 1997
19. Xie, "Study on mass transfer and turbulence in large pipe flow using limiting current density technique", MS thesis – Ohio university, Athens, 1997

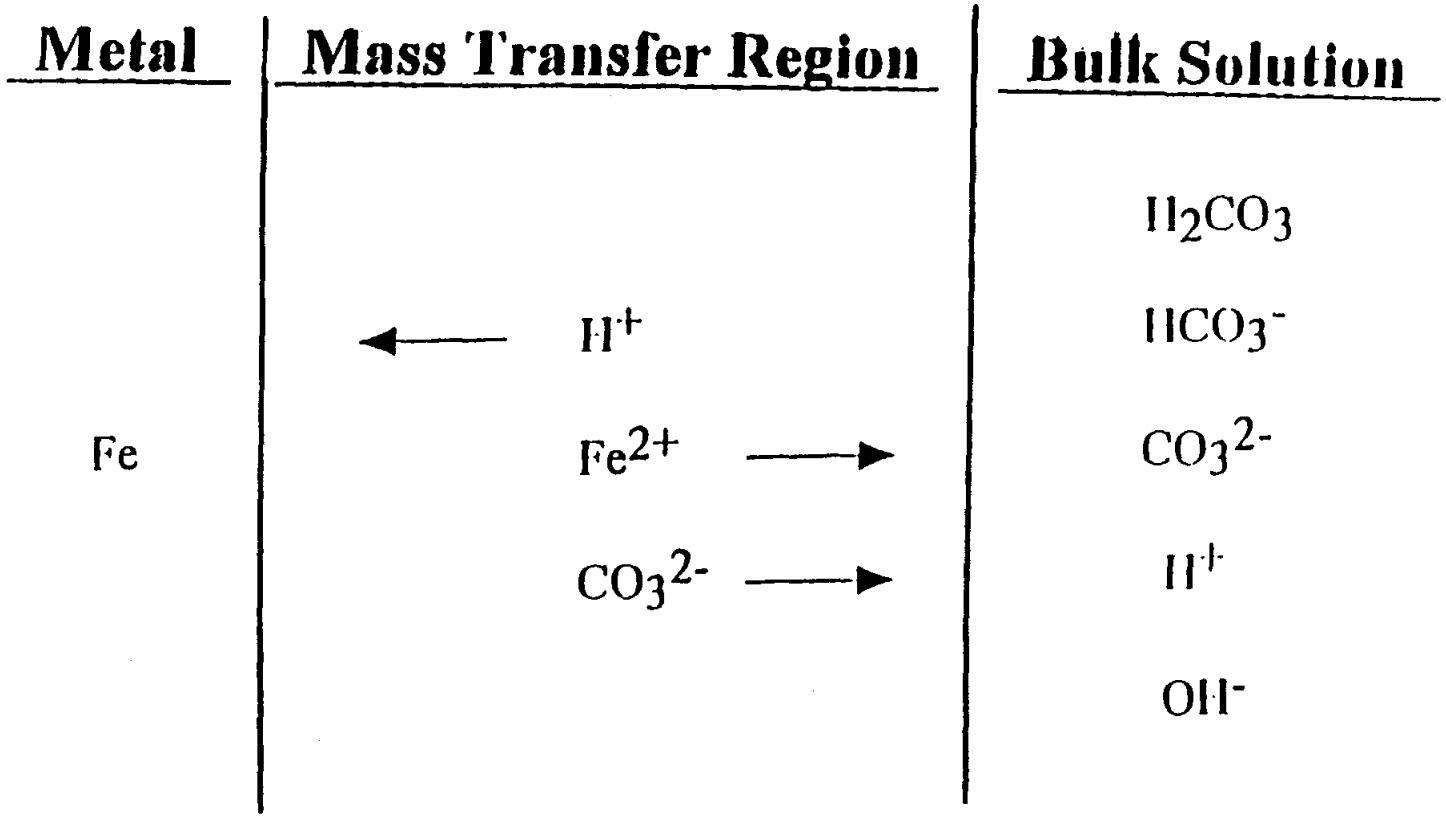

Figure 1. The transfer of ions between the metal surface and the bulk solution

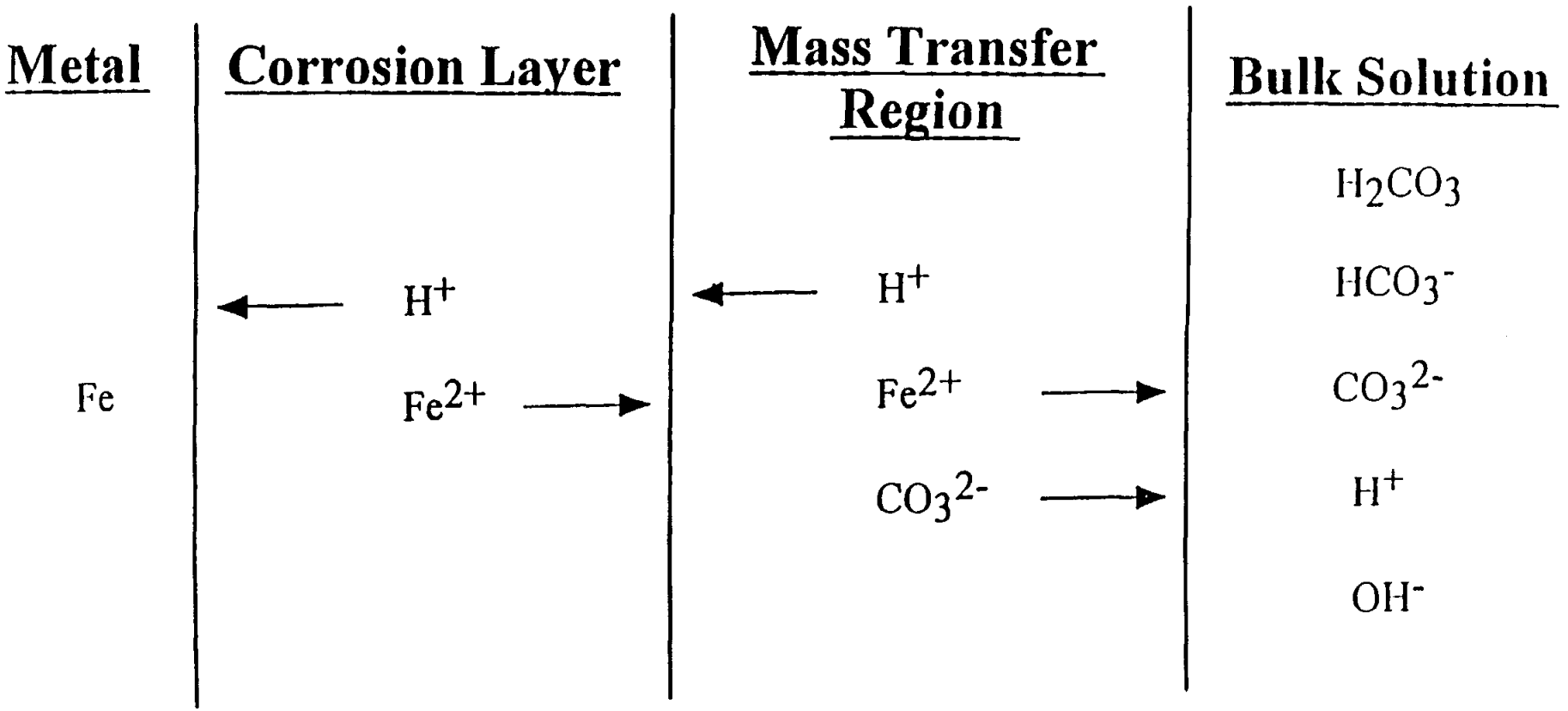

Figure 2. **The effect of a corrosion layer on the transport of ions between the metal surface and the bulk solution**

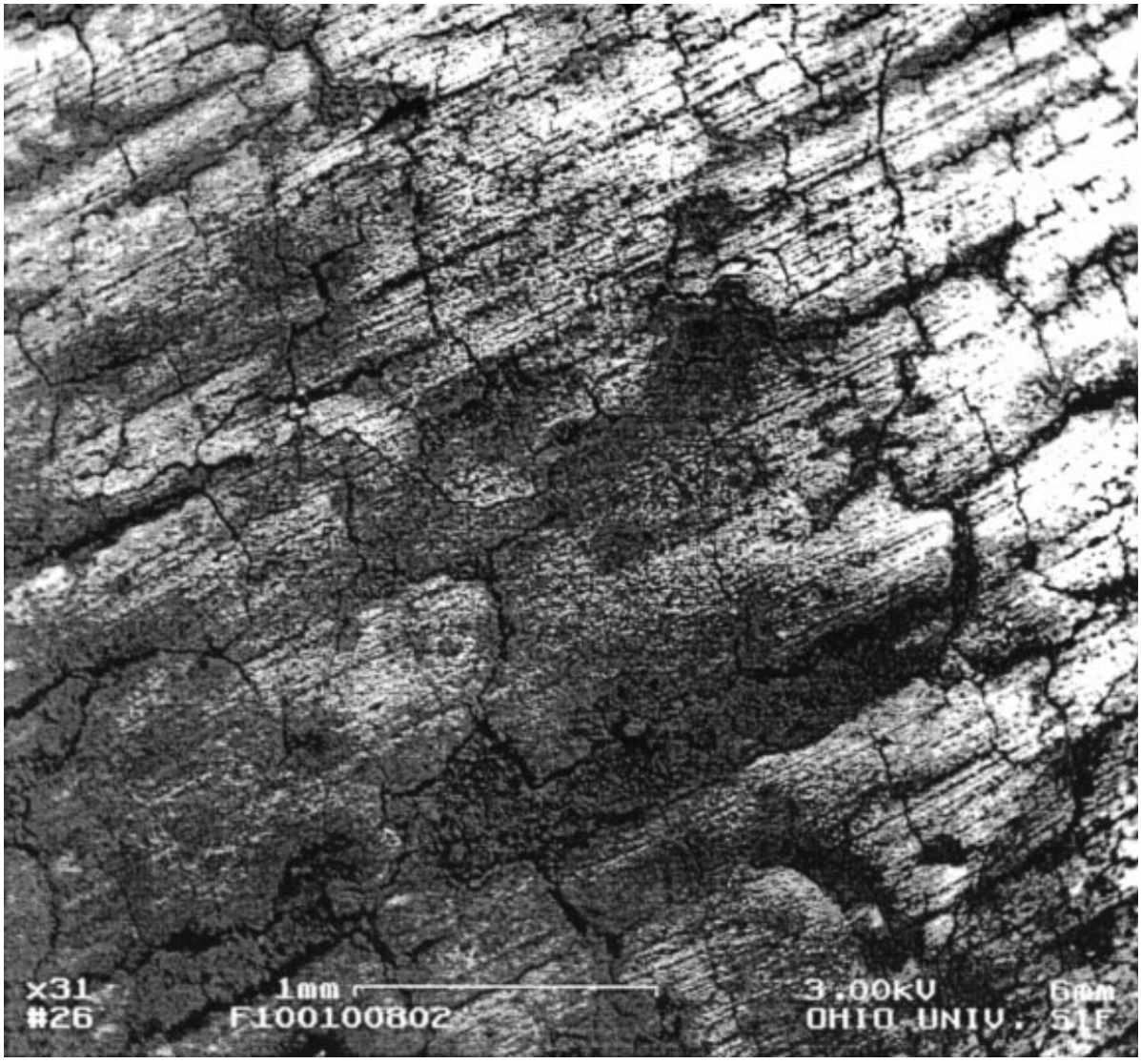

Figure 3. Corrosion film found on the surface of a coupon exposed to full pipe flow conditions (40% Water cut, 80°C, 0.79 MPa and 100 ppm iron concentration).

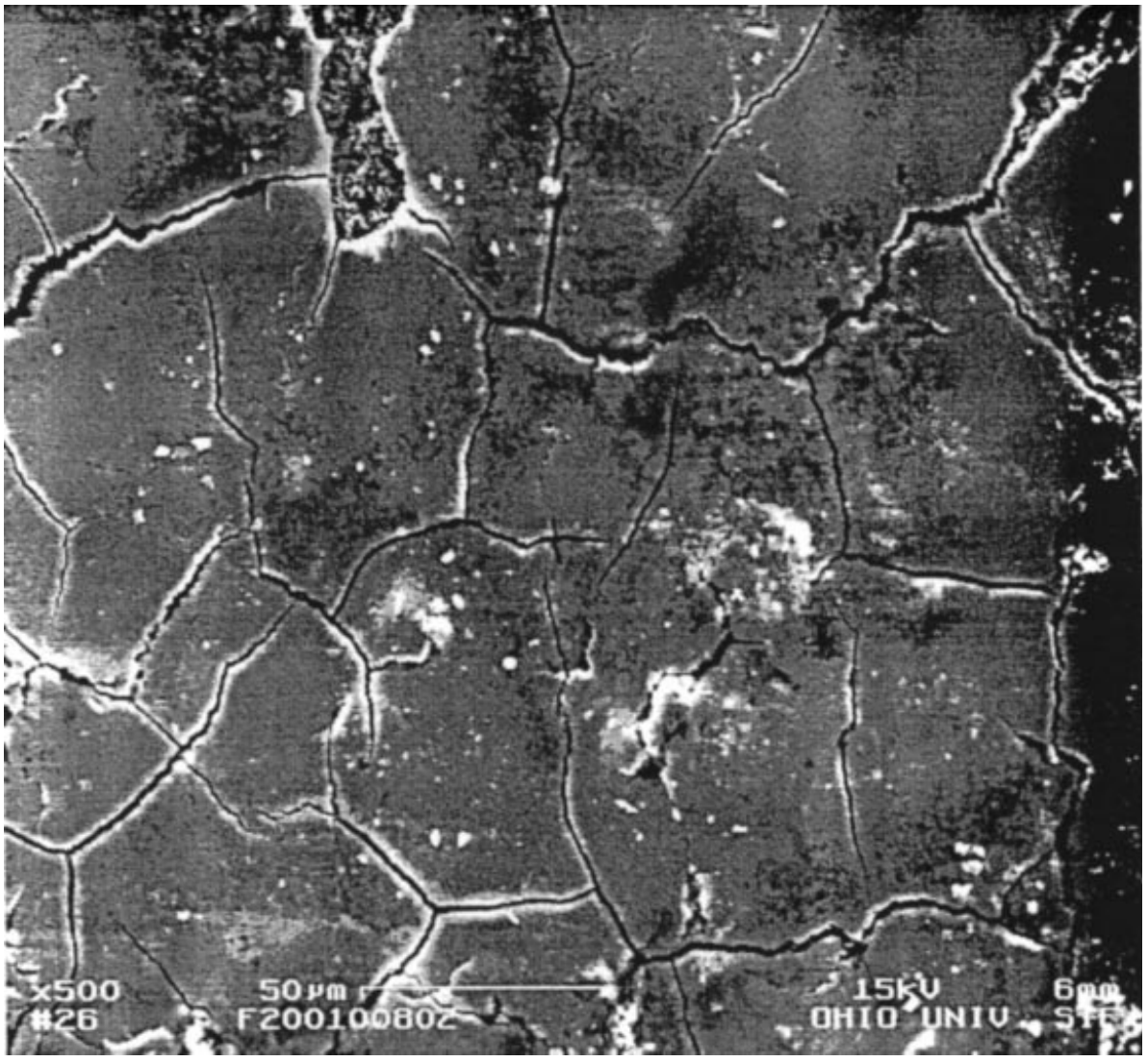

Figure 4. Corrosion film found on the surface of a coupon exposed to full pipe flow conditions (40% Water cut, 80°C, 0.79 Mpa and 200 ppm iron concentration.

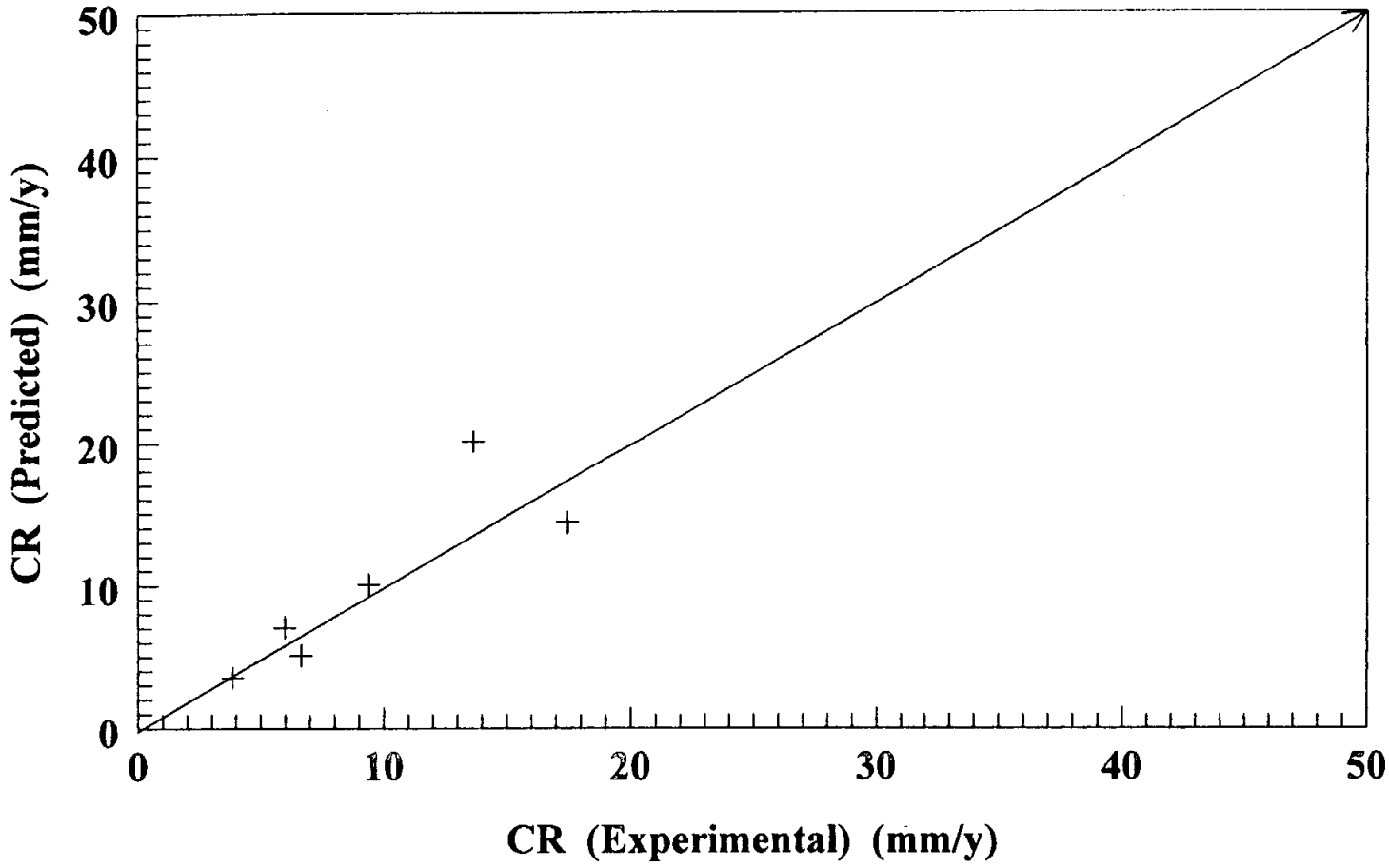

Figure 5: Predicted vs Experimental Corrosion Rates by Using Vieth Expression for 40C (1D)

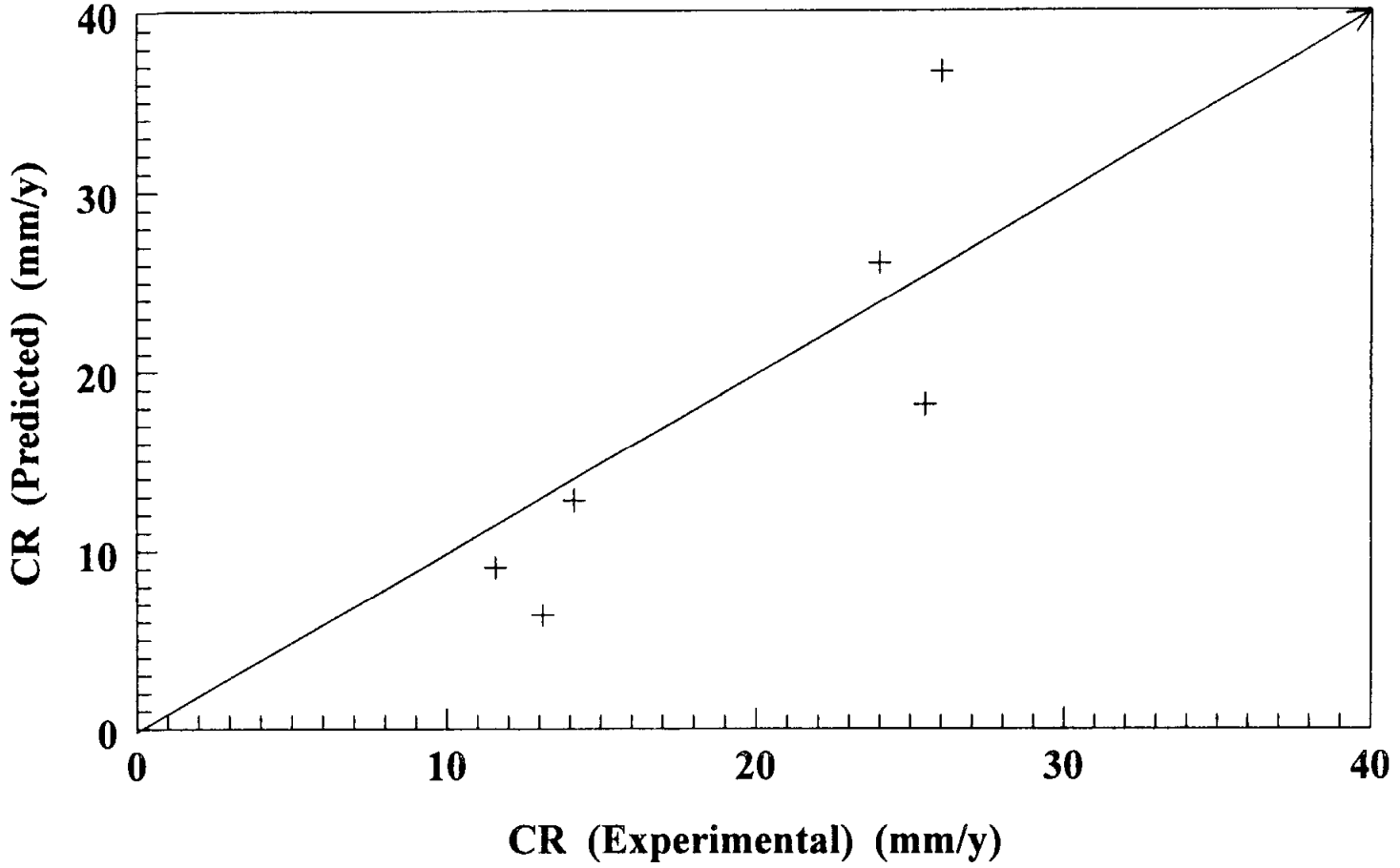

Figure 6: Predicted vs Experimental Corrosion Rates by Using Vieth Expression for 60C (2D)

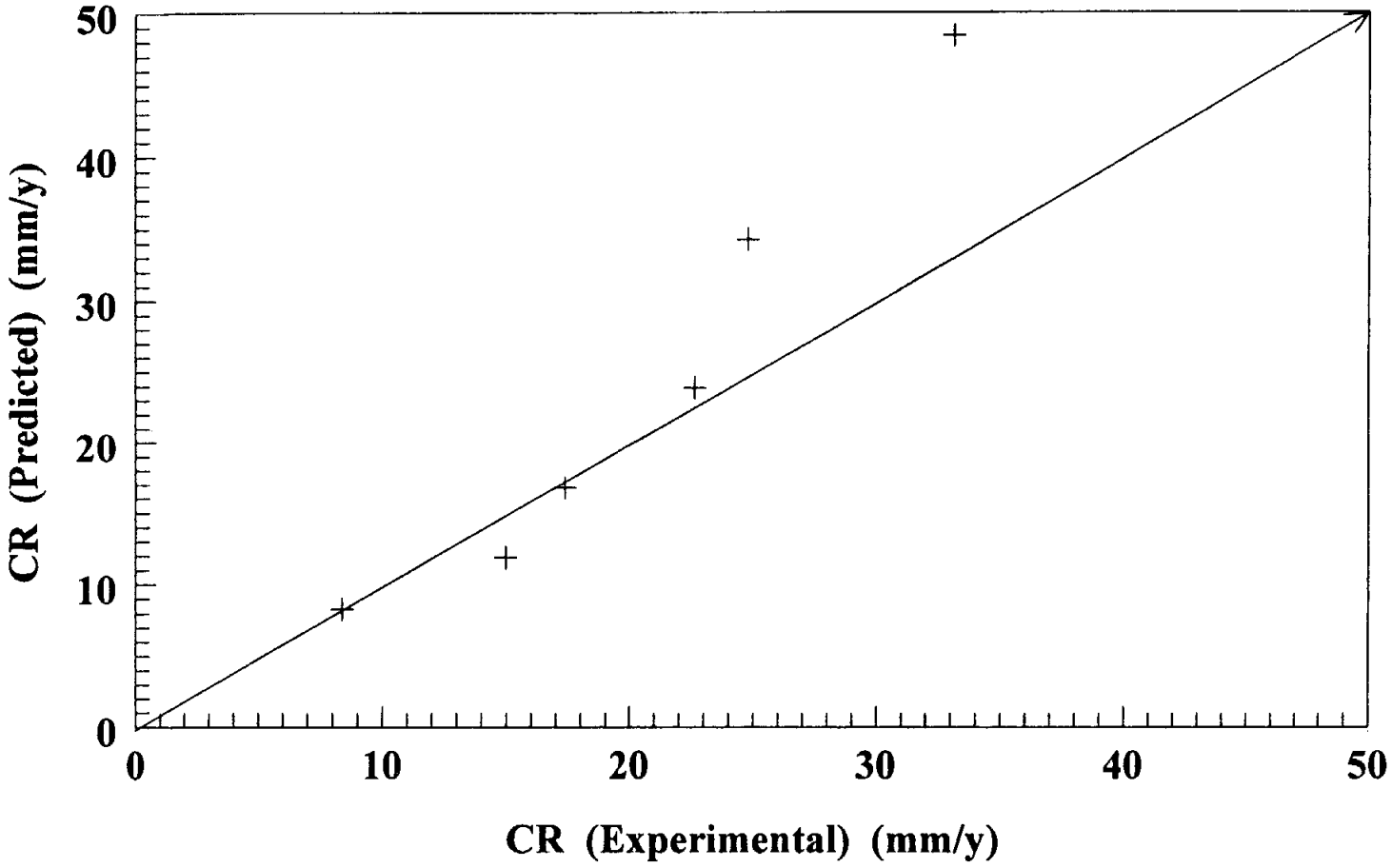

Figure 7: Predicted vs Experimental Corrosion Rates by Using Vieth Expression for 80C (3D)

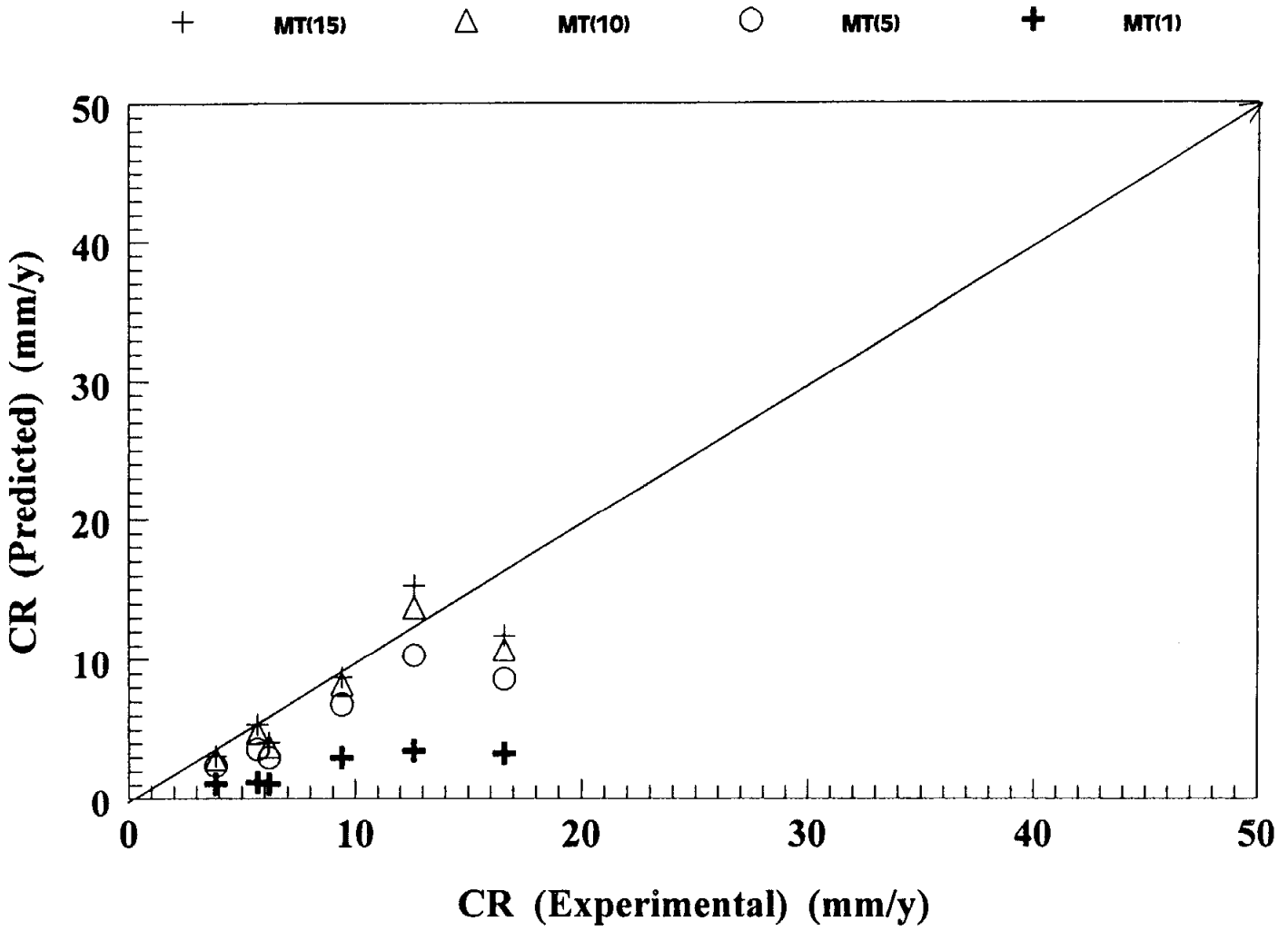

Figure 8: Predicted vs Experimental Corrosion Rates by Using Vieth Expression at 30microns for 40C(1D)

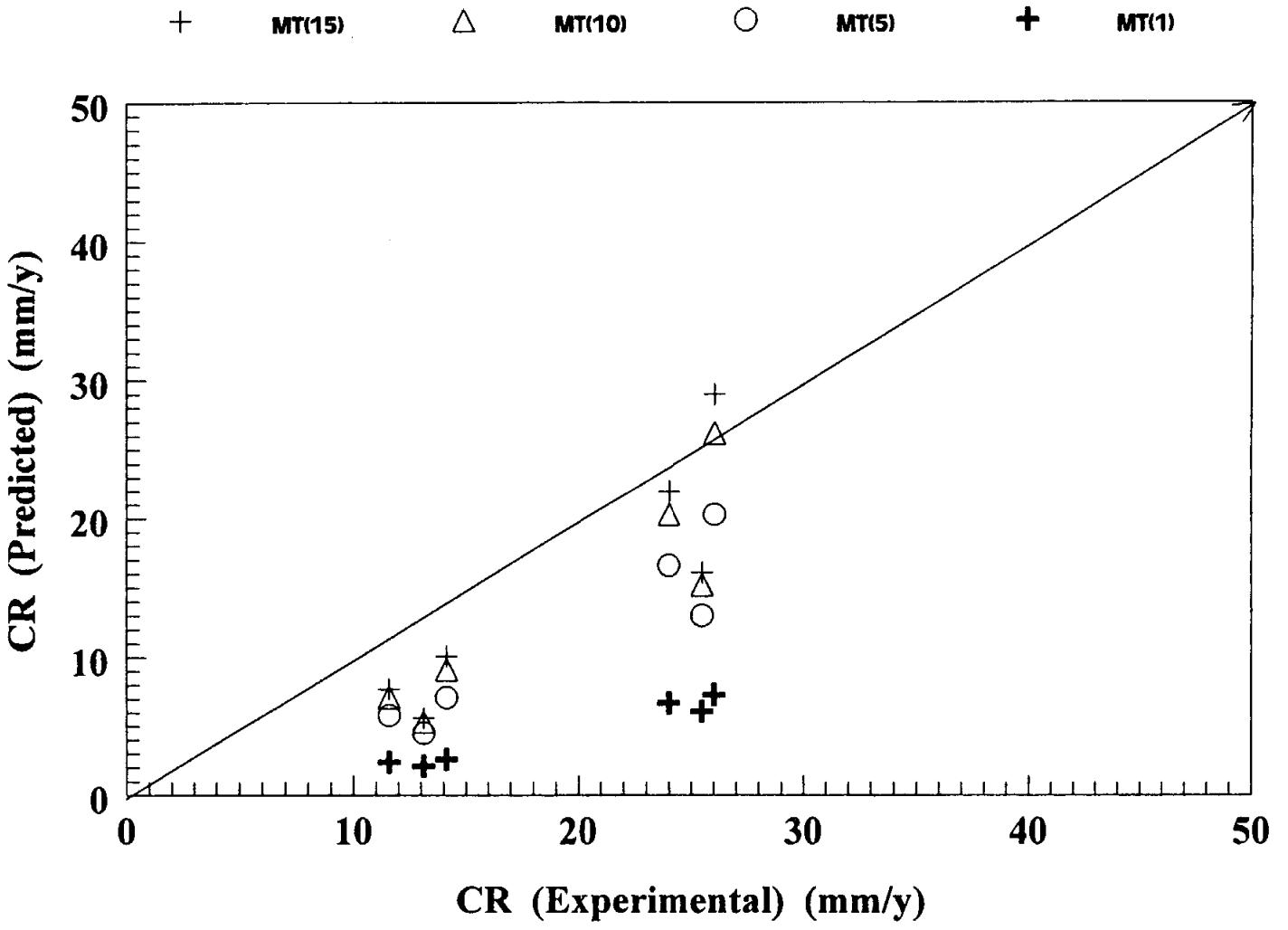

Figure 9: Predicted vs Experimental Corrosion Rates by Using Vieth Expression at 30microns for 60C(2D)

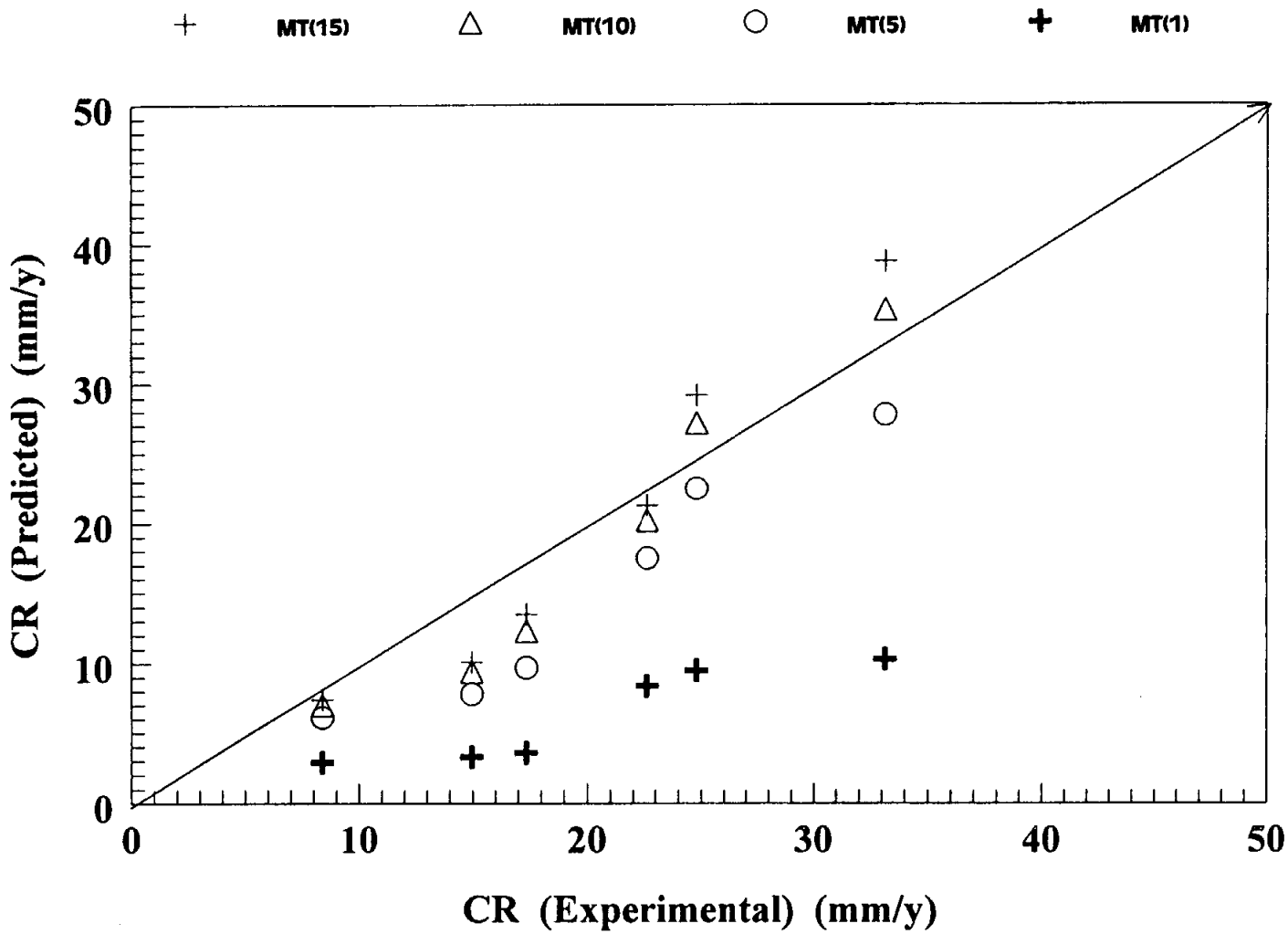

Figure 10: Predicted vs Experimental Corrosion Rates by Using Vieth Expression at 30microns for 80C(3D)

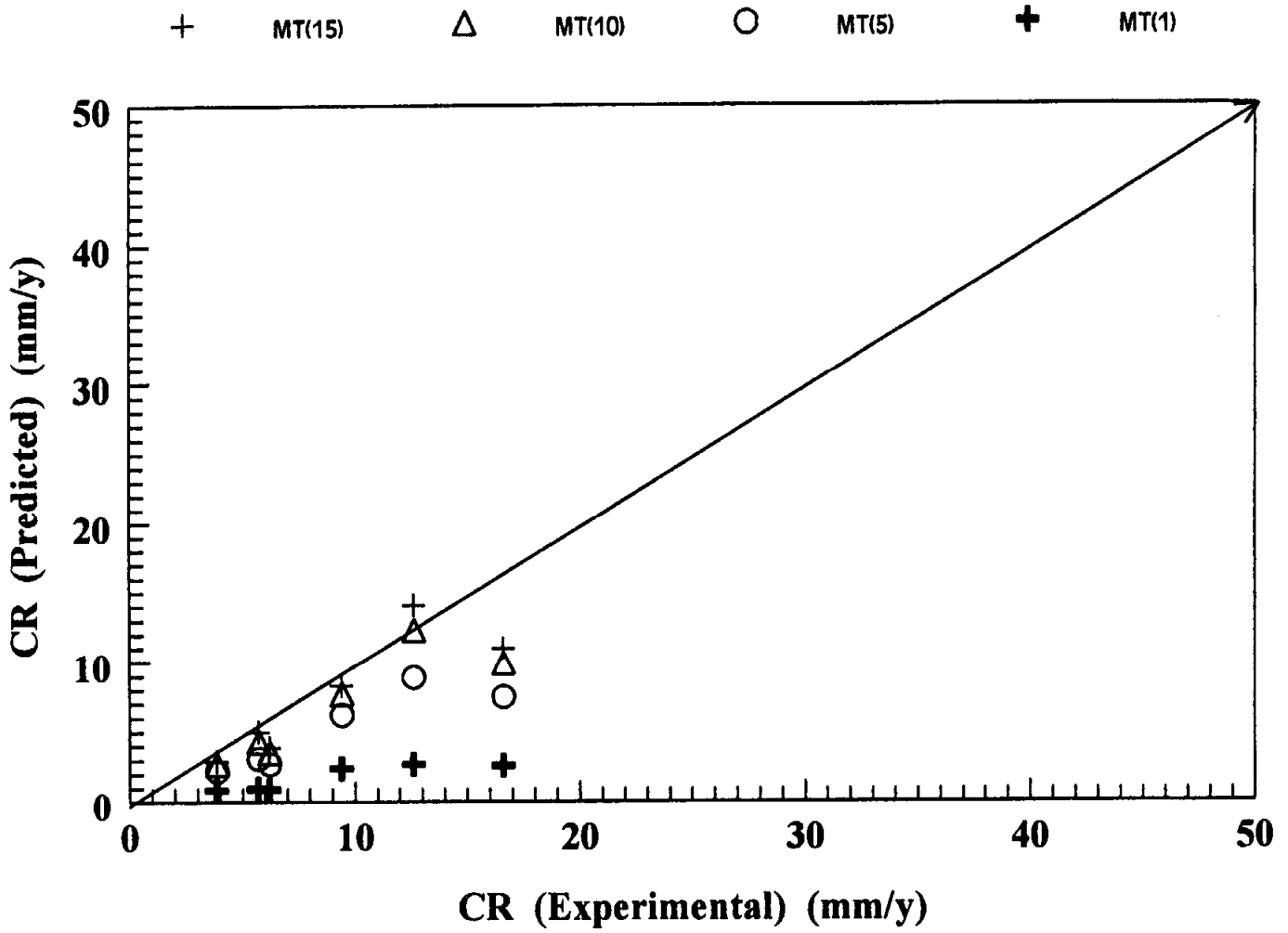

Figure 11: Predicted vs Experimental Corrosion Rates by Using Vieth Expression at 40microns for 40C(1D)

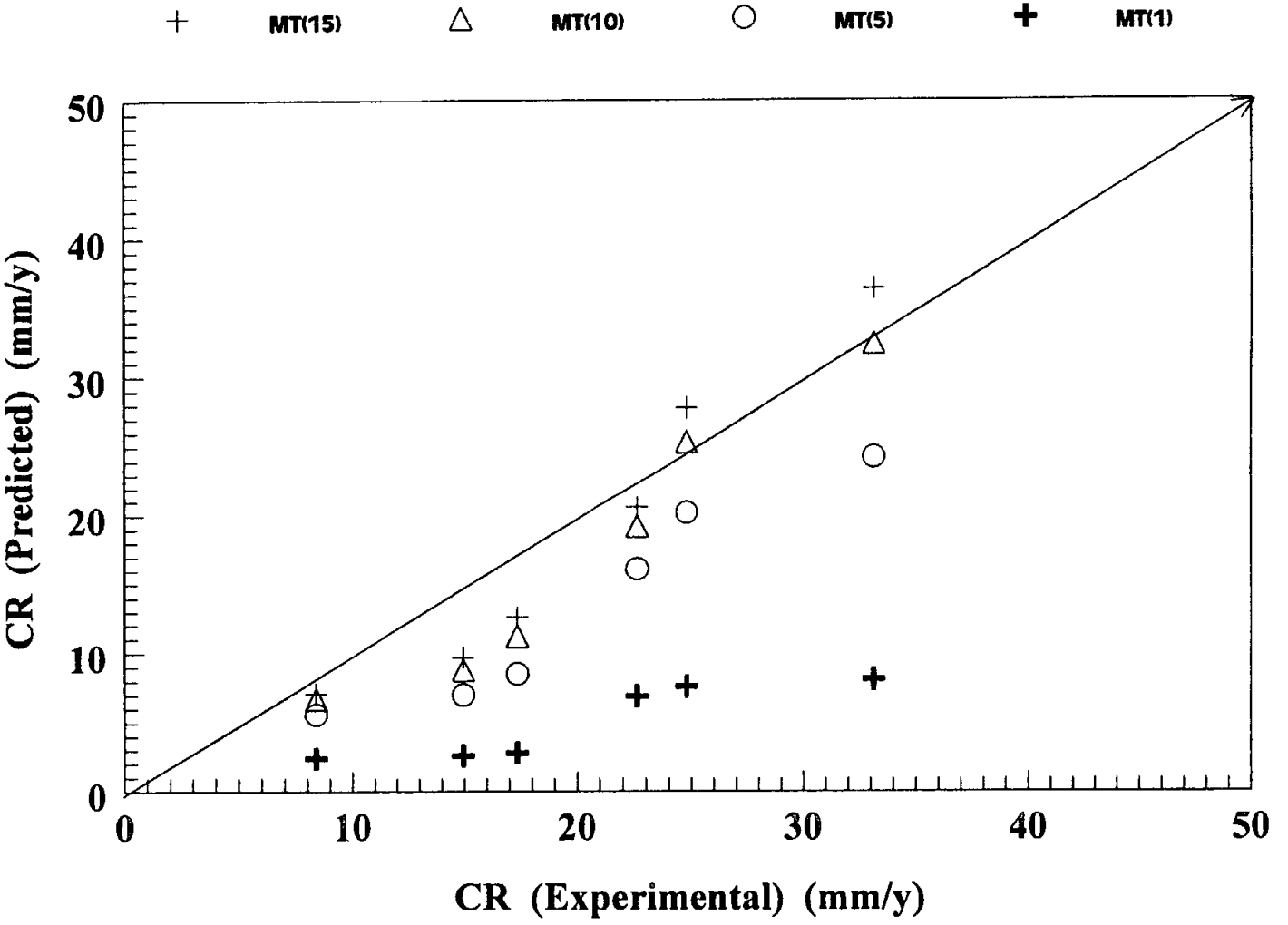

Figure 13: Predicted vs Experimental Corrosion Rates by Using Vieth Expression at 40microns for 80C(3D)

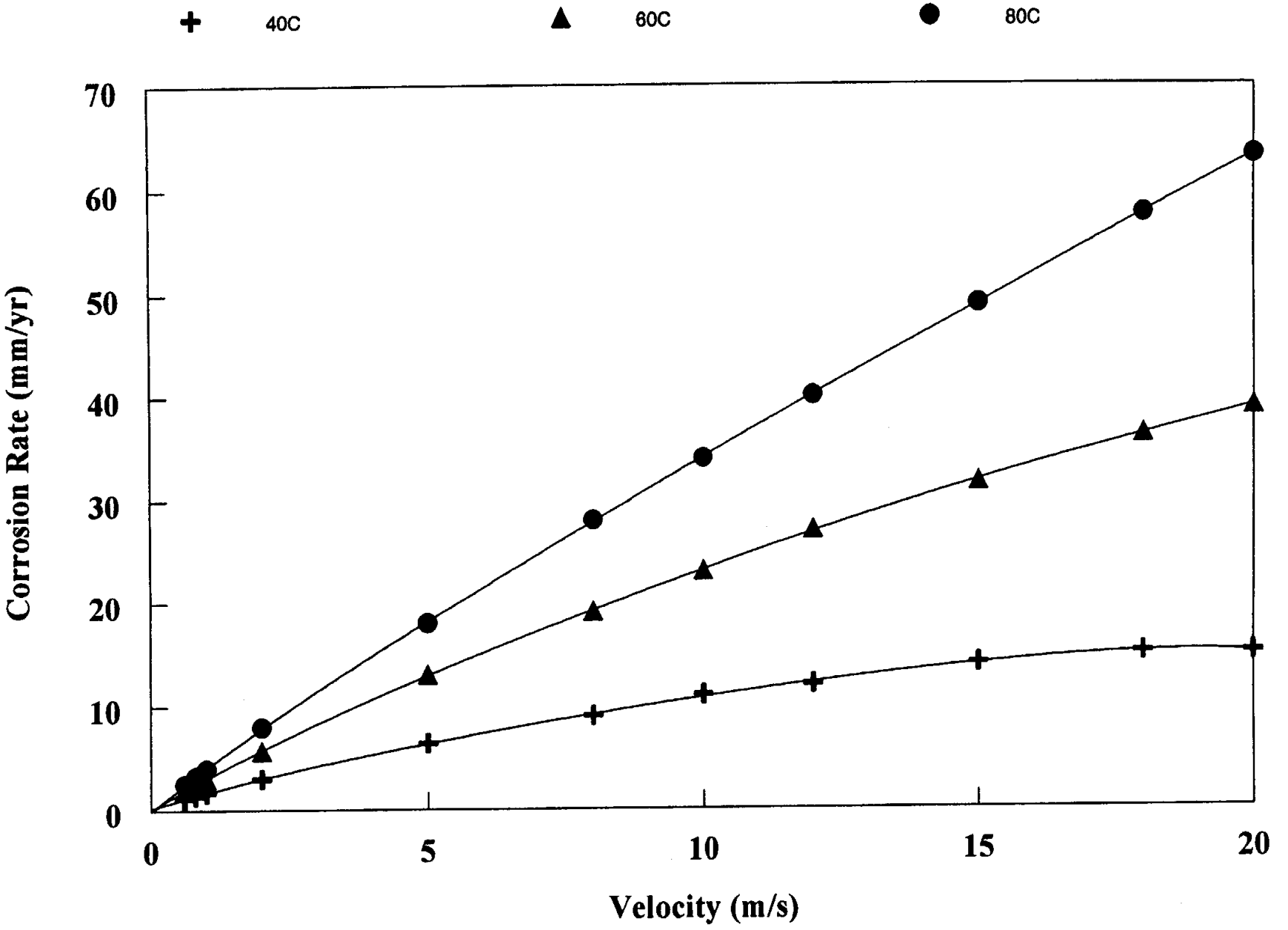

Figure 14: Predicted Corrosion rate vs velocity for 40, 60 and 80C in ASTM seawater at 0.13MPa